DISTRIBUTION STATEMENT A: Distribution approved for public release; distribution is unlimited

Ocean Battlespace Sensing (OBS) S&T Department Annual Report

J.D. Huba
Plasma Physics Division
Naval Research Laboratory
Washington, DC 20275
phone: (202) 767-6863 fax: (202) 767-0631 email: huba@nrl.navy.mil

D. Drob
Space Science Division
Naval Research Laboratory
Washington, DC 20275
phone: (202) 767-6863 email: douglas.drob@nrl.navy.mil

J. Krall
Plasma Physics Division
Naval Research Laboratory
Washington, DC 20275
phone: (202) 767-4416 fax: (202) 767-0631 email: jon.krall@nrl.navy.mil

Award Number: N0001414WX20599
http://www.onr.navy.mil/sci_tech/reports/annual

LONG-TERM GOALS

To understand the influences of acoustic-gravity waves due to seismic events and atmospheric sources on the low- to mid-latitude ionosphere.

OBJECTIVE

The proposed program is to develop a first-principles, physics-based description of the response of the ionosphere to atmospheric gravity waves (AGWs) generated by tsunamis and other geophysical disturbances (e.g., volcanoes, earthquakes).

APPROACH

The approach is to couple the GATS compressible model and the NRL stochastic wave model to the ionosphere models SAMI3 and SAMI3/ESF, and to carry out a detailed investigation of the impact of seismic-generated gravity waves on the ionosphere. A broad parameter range of gravity wave parameters will be considered: wave velocity and density perturbations as a function of altitude, wavelength, frequency, and propagation direction. The key observables to be determined are changes in the ionosphere electron density and temperature, as well as the current system. Finally, we will apply our simulation models to ground-truth event data sets (e.g., ground-based GPS TEC data and/or radar observations).

WORK COMPLETED

The atmospheric spectral wave model developed at NRL was incorporated into the NRL code SAMI3/ESF. Several simulation studies were carried out to assess the impact of the AGWs on the ionosphere. The simulations used geophysical parameters relevant to the 11 March 2011 tsunami and observations made by Makela et al. (2011). Additionally, we have incorporated 3D atmospheric gravity wave data from first-principle simulations performed by GATS, Inc. into SAMI3/ESF. We have initiated a series of simulations using this data focusing on the ionospheric response of the gravity wave propagation angle relative to the geomagnetic field.

RESULTS

We developed a new frequency domain tsunami-driven gravity wave source function that will be implemented in SAMI3/ESF. This source function model can be easily tuned, replaced by more detailed ocean surface perturbation simulations, or even buoy observed waveforms. Figure 1 shows the atmospheric gravity wave response, in terms of the zonal and vertical wind wave perturbation amplitudes, for the waveform shown in Figure 1 assuming a propagation direction of east to west. The magnitude, frequency content, and altitude extent of these perturbations have important consequences for how well the tsunami wave perturbation couple into the ionospheric plasma.

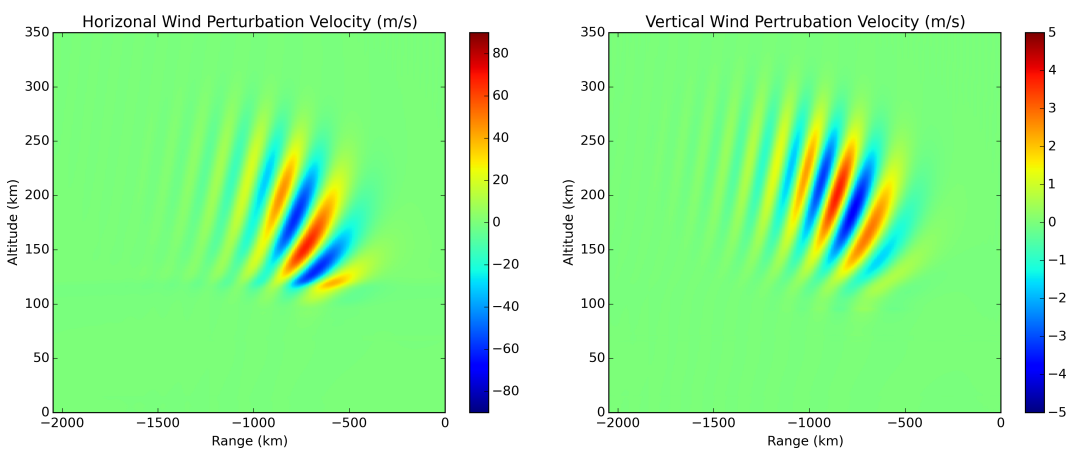

Figure 1: Horizontal and vertical wind perturbations induced by tsunami-driven gravity waves.

We incorporated this new tsunami-driven model into SAMI3/ESF. We ran a number of simulations in which we included gravity waves and did not include gravity waves. We differenced the results of these simulations for several variables (e.g., electron density, ion velocity along **B** to isolate the influence of tsunami-driven gravity waves on the ionosphere.

In Fig. 2 we show contour plots of (a) the gravity-wave induced neutral velocity V_{nq} along **B**, (b) the differential ion velocity ΔV_{iq} along **B**, (c) the ion velocity V_{ip} transverse to **B**, and

(d) the differential electron density Δn_e as a function of latitude and altitude at time 12:44 UT. The modeled tsunami-driven gravity wave propagates from the northern to southern hemisphere in the altitude range 200 - 300 km; Fig. 2a shows the variation in the neutral velocity along $\mathbf{B}$ at $\sim 20°$. This variation is mirrored in the differential ion (O^+) velocity ΔV_{iq} (Fig. **??**b) and is a direct result of the ion-neutral collisional coupling in the lower ionosphere. Additionally, neutral wind variations transverse to $\mathbf{B}$ generate an electric field that produces an $\mathbf{E} \times \mathbf{B}$ drift of the plasma. Figure 2c shows the $\mathbf{E} \times \mathbf{B}$ velocity V_{ip} transverse to $\mathbf{B}$ in the latitude-altitude plane where positive (red) is outward and negative (blue) is inward. This drift maps to the conjugate region (i.e., southern hemisphere) because the magnetic field lines are equipotentials to lowest order. Thus, even though the gravity wave disturbance is in the northern hemisphere, it can affect the ionosphere in the southern hemisphere.

This last point is shown in the Fig. 2d which is the differential electron density. The largest perturbations in the electron density are localized in the region of the gravity wave ($\theta \sim 18° - 22°$ in the altitude range 200 - 300 km); in this region the color table is saturated and the density variation is $\sim \pm 4 \times 10^4$ cm^{-3}. The large variations in this region are primarily caused by the ion-neutral coupling along $\mathbf{B}$. However, the electron density variations above $\sim$ 400 km in the northern hemisphere and those in the southern hemisphere are driven completely by the $\mathbf{E} \times \mathbf{B}$ velocity V_{ip}. The electron density variation is dependent on $\mathbf{V}_{ip} \cdot \nabla n_e$. The F-peak is at $\sim$ 350 km; the change in sign of the electron density variation along $\mathbf{B}$ from below the F-peak to above the F-peak occurs because the sign of ∇n_e changes from positive to nega-

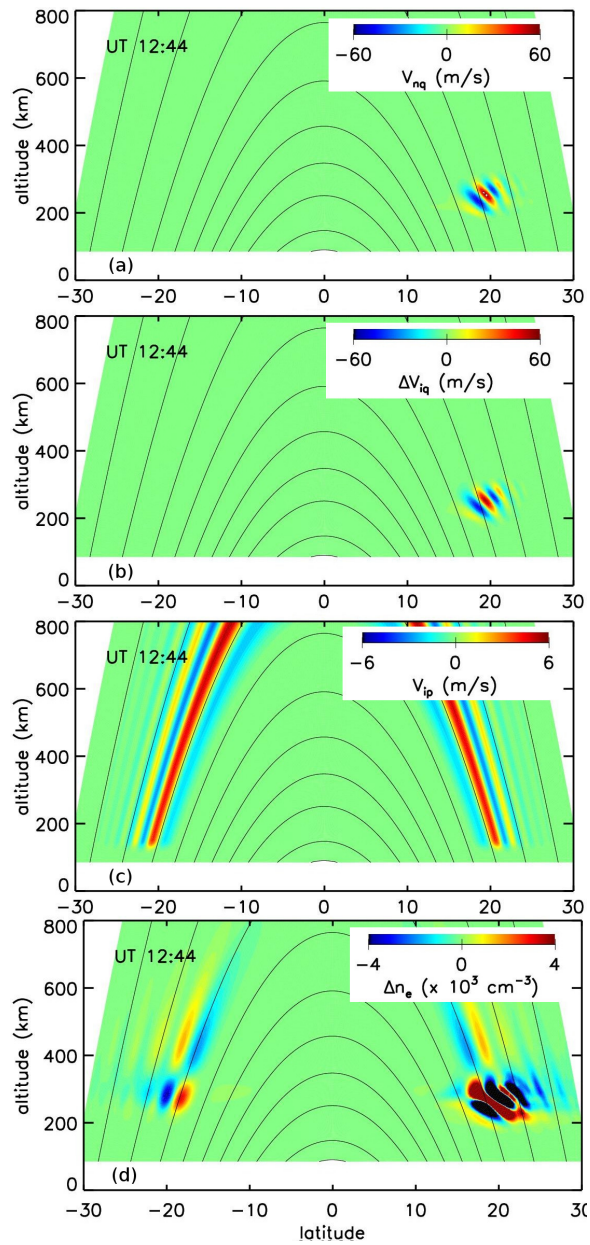

Figure 2: Contour plots of (a) the gravity-wave induced neutral velocity V_{nq} along $\mathbf{B}$, (b) the differential ion velocity ΔV_{iq} along $\mathbf{B}$, (c) the ion velocity V_{ip} transverse to $\mathbf{B}$, and (d) the differential electron density Δn_e as a function of latitude and altitude at time 12:44 UT.

tive.

We compared observational and simulation results of the percentage difference in the 6300Å airglow between the gravity wave disturbed ionosphere and the background ionosphere in Fig. 3. The data plot is at time 12:58 UT (same as Fig. 1 in Makela et al. (2011) and longitude $\sim 160°$ W. It is generated by dividing the filtered wave image by the background-subtracted image and multiplying by 100 (this assumes a linear mapping from counts to Rayleigh). The simulation data is the percentage difference between the wave and non-wave simulation results for the 6300Å and is at time 13:12 UT. The slight offset in time between the observational and simulation data is done to align the zero points at $\sim$ 200 km. The simulation results agree reasonably well with the data. The amplitude of the maximum variation of the simulation data is smaller than the observations, and the wavelength of the variation is somewhat larger. Additionally, we also show the vertical displacement of the ocean surface [Eq. (1)] as a function of distance where we offset the maximum displacement to correspond to the maximum observed airglow perturbation.

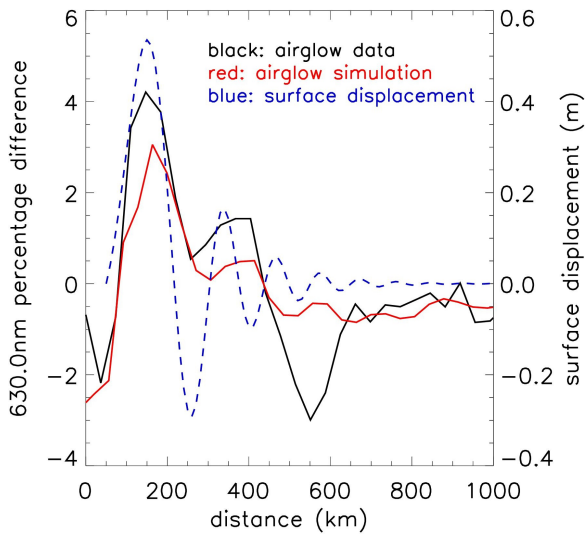

Figure 3: Data and simulation comparison of the percentage difference of 6300Å emission between the gravity wave disturbed ionosphere and the non-disturbed ionosphere as a function of distance.

Lastly, we have recently incorporated gravity wave data from first-principles simulation results from GATS, Inc. into SAMI3/ESF. We have initiated a series of simulations using this data . The main focus of this effort is to understand the effects of gravity wave propagation relative to the direction of the geomagnetic field on the ionosphere. Preliminary results suggest that the conjugate effect discussed above is highly dependent on propagation direction.

IMPACT/APPLICATIONS

Potential impact is to provide information regarding the source of the atmospheric disturbance (e.g., location, magnitude, type).

TRANSITIONS

This research has been used in a project funded by DTRA to understand and model the possible impact of underground nuclear and above ground chemical explosions on the ionosphere.

RELATED PROJECTS

This project is related to a NASA research grant (PI: J.D. Huba) to study the impact of gravity waves on the initiation of equatorial spread F.

REFERENCE:

Makela, J.J. et al., *Geophys. Res. Lett. 38*, L00G02, doi:10.1029/2011GL047860, 2011.

HONORS/AWARDS/PRIZES

Dr. J.D. Huba was elected Fellow of the American Geophysical Union (2013).

PRESENTATIONS/PAPERS:

Huba, J.D., D.P. Drob, T.-W. Wu, and J.J. Makela, Modeling the ionospheric impact of tsunami-driven gravity waves with SAMI3: Conjugate effects, *Geophys. Res. Lett., 42*, 5719, doi:10.1002/2015GL064871, 2015.

Huba, J.D., D. Drob, and T.-W. Wu, Impact of tsunami-driven gravity waves on the ionosphere, presented at the 2014 Fall AGU Meeting, San Francisco, CA, 2014.

Huba, J.D., Tsunami-driven gravity wave effects on the ionosphere, presented at the BRC Science Meeting, Boulder, CO, 2015.